

# TOPOLOGICAL LANDMARK-BASED NAVIGATION AND MAPPING

R. GHRIST, D. LIPSKY, J. DERENICK, AND A. SPERANZON

ABSTRACT. Algebraic-topological criteria for domain coverage, hole-detection, and mapping are given in the context of dynamic multi-agent systems navigating with respect to beacons or landmark visibility. The key constructs involve dual pairs of nerves of the relevant visibility and observation covers, based on a sensing relation, either binary or via distance/signal-strength. This, in turn, is used to construct simplicial approximations to the regions explored as a topological map of the domain. We prove equivalence of various simplicial approximations (based on landmarks or observation points), show how to incorporate distance-correlated data with persistent homology, and demonstrate these methods via simulations.

## 1. INTRODUCTION

Imagine a lost traveler wandering through winding, convoluted streets in an unfamiliar city with unreadable street signs. Such a traveler might use various landmarks to build up an internal map: *“From the jewelry store, walk toward the cafe with the red sign, then look for the tall church steeple.”* This can be accomplished without reference to coordinates or odometry — even directions such as *“turn left”* may be foregone. Though it seems clear that such non-metric qualitative descriptors can abstractly lead to a rough map, the mathematics behind this procedure and its integration with quantitative structure are not obvious. This paper proposes several appropriate mathematical constructs, proves an equivalence result between them (using a certain topological duality) and demonstrates relevance to a variety of localization and mapping contexts.

Figure 1 encapsulates the main constructions of the paper in a simple example. A planar domain  $\mathcal{D}$  is filled with landmarks (in this case, corners of  $\mathcal{D}$ ) identifiable by observers that register landmarks via local line-of-sight visibility. A collection of observations are taken, with each observation recording only those landmarks “visible” from the observation point. Both the landmarks  $\mathcal{L}$  and observations  $\mathcal{O}$  are each a discrete set, with no geometric or coordinate data appended. The sensing data is given in the form of a subset  $\mathcal{R} \subset \mathcal{O} \times \mathcal{L}$  — an unordered sequence of pairs of observation-landmark points encoding who-sees-what. From this abstract data, we detail (in §5) a pair of simplicial complexes: the **landmark complex**,  $\mathcal{K}_{\mathcal{L}}$ , having as vertices landmark points, and the **observation complex**,  $\mathcal{K}_{\mathcal{O}}$ , having as vertices the observation points: see Figure 1.

One notes from the figure that these complexes are accurate topological approximations to  $\mathcal{D}$ : the connectivity and holes in the complexes match those of the underlying domain  $\mathcal{D}$ . This fidelity to  $\mathcal{D}$  is variable and a function of the number, type, and placement of observations and landmarks in  $\mathcal{D}$ . What is certain is the topological equivalence of these dual approximations. We prove in §5 that  $\mathcal{K}_{\mathcal{L}}$  and  $\mathcal{K}_{\mathcal{O}}$  are topologically equivalent, and, with further assumptions, equivalent to certain “coverage” regions in  $\mathcal{D}$ . As can be seen from Figure 1, these complexes are of different “size” and one is often computationally simpler than the other, demonstrating one of the applications of our duality result.

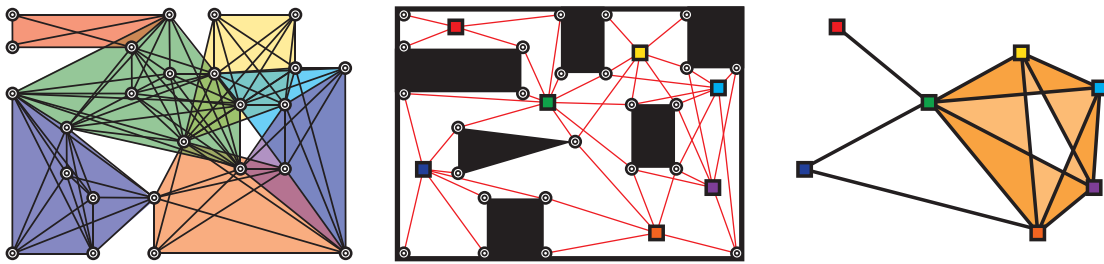


FIGURE 1. A collection of observations (center, squares) taken by a moving observer or multiple communicating observers, register the presence of identifiable landmarks (center, circles) in a planar domain  $\mathcal{D}$  via line-of-sight observations. The resulting simplicial complexes, the landmark complex  $\mathcal{K}_{\mathcal{L}}$  (left) and the observation complex  $\mathcal{K}_{\mathcal{O}}$  (right), approximate  $\mathcal{D}$  using two different vertex sets. Although the figures are drawn geometrically, no coordinate information is assumed or used in the construction of the complexes.

## 2. PROBLEM FRAMEWORK

This paper considers the following setting for landmark-based coverage, navigation, and mapping in an unknown environment. Given a collection of identifiable landmarks in a domain (landmarks assumed static, for the time being), assume that one or more vehicles can navigate without GPS information by localizing coarsely with respect to a collection of locally-detectable landmarks. We consider the problems of how to infer domain topology/geometry, localize holes, and navigate so as to fill-in such holes, as one or more vehicles navigates through the domain without the benefit of coordinates, distances, or bearings.

In what follows, we use ‘visibility’ and ‘visible’ as a shorthand for sensing. This includes but does not restrict to the setting of optical- or vision-based sensing. Other sensing modalities fit into this framework, so long as the assumptions (below) about detection and convexity hold. We stress that no need for signal strength, range, bearing, or other descriptor is needed: our sensing model for landmark detection is purely

binary. Although data about the environment is collected by mobile agents, no temporal data is required: neither synchronization nor clocks are requisite.

The following assumptions and notations will be used throughout the remainder of this work:

- (A1): Let  $\mathcal{D}$  be a connected, tame Euclidean domain, perhaps with boundary.
- (A2): A collection of labeled landmarks  $\mathcal{L}$  can be sensed (“are visible”) by agents. The landmarks have a geometric representation as  $|\mathcal{L}| \subset \mathcal{D}$ .
- (A3): A collection of labeled observations  $\mathcal{O}$  are taken. The points of observation have a geometric representation as  $|\mathcal{O}| \subset \mathcal{D}$ .
- (A4): The ability of agents to detect landmarks is encoded as a relation  $\mathcal{R} \subset \mathcal{O} \times \mathcal{L}$ , in which  $(\alpha, i) \in \mathcal{R}$  iff observation  $\alpha \in \mathcal{O}$  detects landmark  $i \in \mathcal{L}$ .

To emphasize, the sets  $\mathcal{L}$  and  $\mathcal{O}$  are abstract sets, whereas  $|\mathcal{L}|$  and  $|\mathcal{O}|$  are discrete subsets in  $\mathcal{D}$  with specific (albeit unknown) coordinates.

A few of the above assumptions may be bent. For example,  $\mathcal{D}$  can in some cases be relaxed to being a locally-compact geodesic metric space of curvature bounded above, so long as a sensible notion of local convex hull is defined. (The interested reader is referred to the literature on Alexandrov geometry [5] for examples and details of geodesic metric spaces and curvatures thereof.) The requirement that sensing be 0-1 (detect or no-detect) may also be relaxed to a real number  $\mathcal{R}(\alpha, i) \in [0, 1]$ , connoting either signal strength, distance, or certainty of detection. These weights may either be thresholded or incorporated *en masse* via persistence methods: cf. §7.

We use simplicial and homological methods to infer, to such extent as is possible, the qualitative features of the domain  $\mathcal{D}$ , based only on the abstract observations recorded in  $\mathcal{R}$ . There is no assumption that the geometric realizations  $|\mathcal{L}|$  or  $|\mathcal{O}|$  are known — all data is abstracted away from coordinate representations. This is accomplished through the use of **nerves**: see §4 for definitions.

### 3. EXISTING WORK

The principle tool of this paper — nerves — are by no means new. Dowker’s Theorem on homology of relations (using nerves, without that terminology) is from 1952 [14]. The Nerve Theorem of Leray is from 1945 [24], though the basic form of the result (enough for the applications of this paper) seems to have been known to Čech in the 1930s [7] and Alexandrov earlier than that [1]. Applications of nerves in computational and combinatorial geometry are not uncommon [4, 29]; more recent applications to neuroscience [10], localized camera systems [25], and sensing [19] have helped cement this tool as one of fundamental importance in applications of topology.

The observation complex construction of this paper can be viewed as a more general form of **witness complex**, introduced by Carlsson and de Silva [11] in the context of point-cloud data. Given a set of points  $X \subset \mathbb{R}^n$ , the witness construction chooses a (small) subset  $A \subset X$ , and the witness complex becomes a simplicial complex having

$A$  as vertex set, with simplices filled in if there is a ‘witness’ in  $X$  close enough to the corresponding subset of  $A$  (see [11] for a proper definition, along with several variants — weak, strong, etc.). The constructions of this paper generalize witness complexes to arbitrary sensing relations (not distance-based exclusively) and allow for a more abstract differentiation between the landmark and observation points.

The duality results that we prove are at heart due to Dowker [14] from the 1950’s (assuming their origins are not older still). This type of data structure, along with an image of the duality implicit, has several variants. For the case of finite sets of landmarks (with observation points drawn from these), the sensing relation we use is a so-called **hypergraph** and the resulting nerve is a geometric realization thereof. For the case of a finite set of observations with infinite (subsets of  $\mathbb{R}^n$ ) families of landmarks, similar ideas have arisen independently in computational geometry, in the form of **range spaces** [21] (though the simplicial structures do not appear to have been utilized). Dowker’s results have found sociological and biological network applications via Atkin’s **Q-analysis** [2, 3].

Our intended applications are to multi-agent exploration, including mapping and localization in an unknown environment, in the context of minimal coordinate-free sensing. Recovering the pose of a mobile observer as well as a map of the environment in which it operates is known as the Simultaneous Localization and Mapping (SLAM) Problem [34]. Its roots can be traced back to the seminal results of [8, 23]. In general, SLAM requires a statistical model of landmark detection (i.e., an observation model) and a model describing the observers motions (i.e., a state model). From current measurements and from the previous state estimate prediction, a new refined state estimate is computed for the observer (e.g., its position, attitude, rates, etc.) and its map. Not surprisingly, SLAMs applications are diverse, and it has been leveraged for tasks including coal mine mapping [22], cooperative multi-floor exploration of office buildings [30], and even underwater navigation [17]. Standard approaches are EKF or PF-based depending on the degree of non-linearity of the observation and state models and their statistical properties (Gaussian or non-Gaussian noise), see for example [26, 15]. Approaches bearing the moniker ‘topological’ also exist [32, 9]; however, in the context of SLAM, topology has almost always been taken to mean an embedded graphical representation of the free-space in which locations (rooms, corridors, etc.) are nodes and edges represent the free-space between those elements. Such nodes and edges could also be annotated leading to a fingerprint for the environment [33].

Akin to said approaches, the results presented herein may be interpreted as a solution to a *homological* SLAM problem in which the map is represented as a cellular complex that is iteratively constructed from local observations of abstract features/landmarks.

#### 4. TOPOLOGICAL BACKGROUND

A few brief definitions may be useful to the reader unfamiliar with topological methods. What follows can be found in [16] with a comprehensive treatment in [20]. Experts may proceed to §5.

**SPACES:** A **topological space** is a set  $X$  outfitted with a **topology**, a listing of all open subsets of  $X$ . A topology must be closed under finite intersection and arbitrary union, and must contain both  $X$  and the empty set. Most concepts familiar from basic analysis — continuous mappings, boundaries, convergence sequences, etc. — can be translated cleanly into the setting of topological spaces. Throughout, any use of the term **map** or **mapping** between spaces implies continuity.

**EQUIVALENCE:** Two topological spaces  $X$  and  $Y$  are **homeomorphic** if there exist mappings  $f : X \rightarrow Y$  and  $g : Y \rightarrow X$  with  $f \circ g = \text{Id}_Y$  and  $g \circ f = \text{Id}_X$ . A weaker form of equivalence is more common in topology. Two maps  $f_0, f_1 : X \rightarrow Y$  are **homotopic**, denoted  $f_0 \simeq f_1$ , if there is a continuous 1-parameter family of continuous maps  $f_t : X \rightarrow Y$  extending the pair  $f_0, f_1$ . Two spaces  $X$  and  $Y$  are **homotopy equivalent** (or, simply, homotopic) if there exist maps  $f : X \rightarrow Y$  and  $g : Y \rightarrow X$  such that  $f \circ g \simeq \text{Id}_Y$  and  $g \circ f \simeq \text{Id}_X$ .

**COMPLEXES:** A particularly simple class of spaces with which to work are **regular cell complexes**, consisting of spaces  $X$  built inductively from  $n$ -dimensional skeleta  $X^{(n)}$  via the attachment of  $(n + 1)$ -cells (homeomorphic to the ball  $D^{n+1}$ ), each glued via an injective map  $\partial D^{n+1} \rightarrow X^{(n)}$ . Thus,  $X^{(0)}$  is a discrete set,  $X^{(1)}$  is a topological graph, and  $X = \cup_n X^{(n)}$ . When the attaching cells are **simplices** and the attaching maps affine, respecting the simplicial structure, the cell complex is called a **simplicial complex**; such are geometric realizations of abstract simplicial complexes — collections of finite sets of vertices closed under subsets [27].

**NERVES:** It is a classical problem to approximate the topology of a space  $X$  given a sufficiently good sampling of  $X$ . In the setting of a cover of  $X$  by a collection  $\mathcal{U}$  of subsets  $\{U_\alpha\}$ , the appropriate construct is the **nerve**. The nerve of a cover  $\mathcal{U}$  is defined to be the abstract simplicial complex  $\mathcal{N}_\mathcal{U}$  whose  $k$ -simplices are unordered collections of  $k + 1$  elements of  $\mathcal{U}$  whose intersection in  $X$  is nonempty.

**Theorem 1** (Nerve Lemma [24]). *Let  $\mathcal{U}$  be a **good** cover of  $X$ , meaning that all nonempty intersections of elements of  $\mathcal{U}$  are contractible (including, of course, all  $U_\alpha$ ). Then  $\mathcal{N}_\mathcal{U}$  is homotopic to  $X$ .*

While the assumption of a good (or, more generally, acyclic) cover is nontrivial to verify in general, it is quite a bit looser than the typical metric assumptions about uniform coverage radii, etc. We note that, *e.g.*, all collections of weakly convex sets in a Euclidean space form good covers.

**EULER CHARACTERISTIC:** The simplest topological invariant of a space (besides number of connected components) is the **Euler characteristic**. For a cell complex, the Euler characteristic has a combinatorial definition as the alternating sum of the cells,  $\sigma$ , graded by parity of dimension. Specifically,

$$\chi(X) = \sum_{\sigma} (-1)^{\dim \sigma}. \quad (1)$$

This quantity, when defined, is independent of the cell structure of the space  $X$  and is a homotopy invariant among compact cell complexes.

**HOMOLOGY:** The invariance of Euler characteristic is inherited from its categorification to **homology**. A **chain complex** is a sequence  $C_\bullet$  of vector spaces (or more generally modules)  $C_n$ ,  $n \in \mathbb{N}$ , with linear transformations (resp. homomorphisms)  $d_n : C_n \rightarrow C_{n-1}$  satisfying  $d_{n-1} \circ d_n = 0$  for all  $n$ . The **homology**  $H_\bullet$  of  $C_\bullet$  is the sequence of quotient vector spaces (resp. groups)  $H_n = \ker d_n / \text{im } d_{n+1}$ . The best known example of homology is **simplicial homology**: given a simplicial complex  $X$ ,  $C_n$  has as basis the set of  $n$ -simplices in  $X$  with orientation, and  $d_n$  is the boundary map sending each oriented  $n$ -simplex to its oriented  $n - 1$ -dimensional boundary faces. The resulting homology  $H_\bullet(X)$  is an invariant of the homotopy type of the space  $X$ , and, in particular, is not dependent on the simplicial structure. Euler characteristic can be recovered from homology via  $\chi(X) = \sum_n (-1)^n \dim H_n(X)$ .

**PERSISTENT HOMOLOGY:** A sequence of increasing chain complexes allows one to build a 1-parameter homology. Given a sequence of chain complexes  $C_\bullet^k$ ,  $k \in \mathbb{Z}$ , connected by inclusion maps  $x : C_\bullet^k \hookrightarrow C_\bullet^{k+1}$ , the persistent homology over the parameter range  $[i, j]$  (with  $i < j$ ) is the image of  $H_\bullet(C_\bullet^i)$  in  $H_\bullet(C_\bullet^j)$  via the map  $x^{j-i}$  (the map on homology induced by the composition of  $x$ ). For a filtered simplicial complex  $\emptyset \subset \dots \subset X^i \subset \dots \subset X^j \subset \dots$  the persistent homology  $H_\bullet^{i \rightarrow j}$  has as basis the homology classes in  $X^i$  that remain nonzero under inclusion  $X^i \subset X^j$ . This parametrized homology is particularly useful in settings where a simplicial complex gives an approximation to a structure arising from data, where a length parameter must be specified for connecting proximate data points [6].

## 5. LANDMARK COMPLEXES AND DUALITY

The landmark visibility data  $\mathcal{O}$  can be assembled into a simplicial complex in two distinct ways, using either the landmarks  $\mathcal{L}$  or the observations  $\mathcal{O}$  as the source of vertices. In what follows, assume visibility data in the form of a relation  $\mathcal{R}$  as per Assumption (A4).

**Definition 2.** Given the visibility relation  $\mathcal{R} \subset \mathcal{O} \times \mathcal{L}$ , define the following abstract simplicial complexes:

- (1) The **observation complex**,  $\mathcal{K}_\mathcal{O}$ , is the nerve of the cover of  $\mathcal{L}$  by subsets  $\mathcal{R}_\alpha = \{i \in \mathcal{L} : (\alpha, i) \in \mathcal{R}\}$ , whose  $k$ -simplices are collections of  $(k + 1)$  distinct observations in  $\mathcal{O}$  that have some landmark in common.
- (2) The **landmark complex**,  $\mathcal{K}_\mathcal{L}$ , is the nerve of the cover of  $\mathcal{O}$  by subsets  $\mathcal{R}^i = \{\alpha \in \mathcal{O} : (\alpha, i) \in \mathcal{R}\}$ , whose  $k$ -simplices are all collections of  $(k + 1)$  distinct landmarks witnessed by some observation  $\alpha$ .

Note that according to this definition, only those landmarks that *are observed* participate in the landmark complex; hence it is incorrect to say that, *e.g.*,  $\mathcal{K}_\mathcal{L}$  is a simplicial complex with vertex set  $\mathcal{L}$ , though it is often the case (when all landmarks are observed). Likewise, the observation complex  $\mathcal{K}_\mathcal{O}$  is a simplicial complex with vertex set  $\mathcal{O}$ , or, properly, those points in  $\mathcal{O}$  which see at least one landmark. Such are the caveats of working with abstract simplicial complexes: we emphasize the difference between

the abstract landmarks and observations, and their geometric representations,  $|\mathcal{L}| \subset \mathcal{D}$  and  $|\mathcal{O}| \subset \mathcal{D}$ , within the workspace. There are corresponding geometric realizations of the nerve complexes  $\mathcal{K}_{\mathcal{L}}$  and  $\mathcal{K}_{\mathcal{O}}$  which have a more direct connection to the problems of mapping and navigation.

**Definition 3.** Given the geometric landmarks  $|\mathcal{L}| \subset \mathcal{D}$  and observation points  $|\mathcal{O}| \subset \mathcal{D}$ , define the following Euclidean subspaces:

- (1) The **observation support**  $O_{\alpha}$  of an observation  $\alpha \in \mathcal{O}$  is the convex hull  $\text{cohull}|\mathcal{R}_{\alpha}|$  of landmark points seen by observation  $\alpha$ ;
- (2) The **landmark support**  $L^i$  of a landmark  $i \in \mathcal{L}$  is the convex hull  $\text{cohull}|\mathcal{R}^i|$  of observation points seeing landmark  $i$ .

An observation support  $O_{\alpha} \subset \mathcal{D}$  may be thought of as a navigable set associated to the observation — an approximation to the subspace of  $\mathcal{D}$  from which the observer can navigate to by moving toward immediately visible landmarks. Dually, a landmark support  $L^i \subset \mathcal{D}$  is an approximation to the visibility region associated to the landmark. The union of all observation supports,  $O = \cup_{\alpha} O_{\alpha}$ , and the union of all landmark supports,  $L = \cup^i L^i$ , are approximations to  $\mathcal{D}$  given by observations. It is to be stressed that in the settings we envision, the locations of landmarks  $|\mathcal{L}|$  and observation points  $|\mathcal{O}|$ , are unknown.

To have good control over the topology of the landmark and observation supports, we may impose an additional assumption:

**(A5):** The sensing relation is **local**, by which we mean that the observation and landmark supports satisfy

$$O_{\alpha} \cap O_{\beta} \simeq \text{cohull}(\mathcal{R}_{\alpha} \cap \mathcal{R}_{\beta}) \quad : \quad L^i \cap L^j \simeq \text{cohull}(\mathcal{R}^i \cap \mathcal{R}^j) \quad (2)$$

for all  $\alpha, \beta$  and  $i, j$ .

This assumption rules out behavior in which landmarks “visible” to an observer surround a landmark that is “invisible” (and, dually, observers surrounding a landmark cannot enclose an observer blind to said landmark). Assumption (A5) is valid for many sensing relations that have a strong correlation between detection and distance, such as detection based on a fixed Euclidean distance. See, however, Figure 2 and Figure 6 for non-examples.

The following theorem shows that the landmark and observation complexes and supports all approximate  $\mathcal{D}$  with the same fidelity.

**Theorem 4.** *Under assumptions (A1)-(A5), the following are homotopy equivalent.*

- (1) *The landmark complex  $\mathcal{K}_{\mathcal{L}}$ ;*
- (2) *The observation complex  $\mathcal{K}_{\mathcal{O}}$ ;*
- (3) *The landmark support  $L$ ;*
- (4) *The observation support  $O$ .*

*Without (A5),  $\mathcal{K}_{\mathcal{L}}$  and  $\mathcal{K}_{\mathcal{O}}$  are homotopic, but none of the other equivalences are implied.*

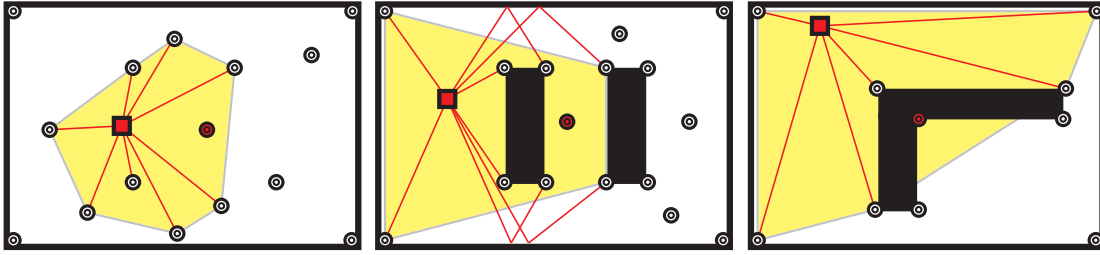


FIGURE 2. Sensing relations with line-of-sight or distance-based tend to be local; those with sensing failures (left), multi-bounce (middle), or certain nonconvex obstacles (right) can be non-local.

*Proof.* The equivalence of  $\mathcal{K}_{\mathcal{L}}$  and  $\mathcal{K}_{\mathcal{O}}$  is immediate from the duality theorem of Dowker [14] for relations. Dowker's theorem states that for  $X$  and  $Y$  sets and any relation  $\mathcal{R} \subset X \times Y$ , the nerve of the columns of  $\mathcal{R}$  on  $Y$  is homotopy equivalent to the nerve of the rows of  $\mathcal{R}$  on  $X$ . In the context of this paper, the dual Dowker complexes of the sensing relation  $\mathcal{R}$  are precisely  $\mathcal{K}_{\mathcal{L}}$  and  $\mathcal{K}_{\mathcal{O}}$ . The remaining equivalences come from the Nerve Theorem, by assigning to  $\mathcal{O}$  the cover generated by observation supports  $\{O_{\alpha}\}$  and to  $\mathcal{L}$  the cover generated by landmark supports  $\{L^i\}$ . From the definitions and Assumption (A5), the nerves of these support covers are precisely  $\mathcal{K}_{\mathcal{O}}$  and  $\mathcal{K}_{\mathcal{L}}$  respectively, since the intersection lattice of observation (or landmark) supports matches that of  $\mathcal{K}_{\mathcal{O}}$  (or  $\mathcal{K}_{\mathcal{L}}$  respectively) via (A5), and convexity of the supports yields an acyclic cover. ■

Note that the resulting complexes are merely approximations to the topology of the portion of  $\mathcal{D}$  surveyed. In particular, certain holes in  $\mathcal{D}$  (perhaps obstacles impenetrable to signals or line-of-sight) can be 'lost' within the complexes of Theorem 4 due to non-acyclicity of the resulting cover: see Figure 3.

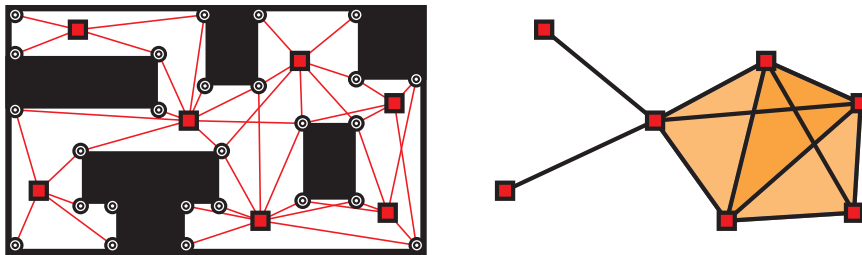


FIGURE 3. A hole in  $\mathcal{D}$  [left] is not detected by the observation complex  $\mathcal{K}_{\mathcal{O}}$  [right], due to observers' ability to 'see' antipodal corners of the hole. The resulting observation and landmark supports likewise eliminate the hole in  $\mathcal{D}$  due to taking convex hulls of sets containing opposite corners of the obstruction.



## 6. EXAMPLES

*Example 5.* Figure 4 gives an example of a disc  $\mathcal{D}$  filled with more than 40 landmarks arranged in an annular shape. This is sampled by 5 observation points. The sensing relation is given in terms of local line-of-sight visibility with irregularly-shaped distance bounds. The complex  $\mathcal{K}_\mathcal{O}$  (pictured, right) is relatively small compared to  $\mathcal{K}_\mathcal{L}$  (not pictured).

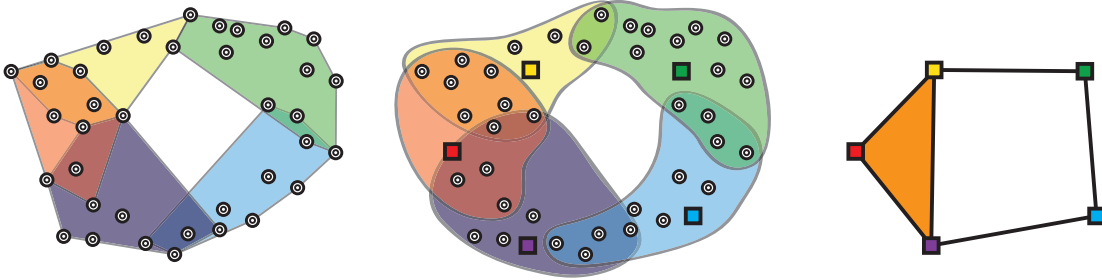


FIGURE 4. Five observations sample a large collection of landmarks via local line-of-sight (center); the observation complex  $\mathcal{K}_\mathcal{O}$  (right) and observation support  $\mathcal{O}$  (left) are homotopy equivalent to the associated landmark complex/support.

*Example 6.* Figure 5 gives an example with 8 landmarks and numerous observation points derived from dense sampling of three continuously-moving agents. The sensing relation is given in terms of line-of-sight visibility with distance bounds. The complex  $\mathcal{K}_\mathcal{O}$  is large and unwieldy, whereas  $\mathcal{K}_\mathcal{L}$  is a very simple complex that approximates the topology of the region explored by the mobile agents **Rob: I must admit that in this example it is not really clear what the topology represents. It clearly depends on the “distance bounds” but those are not depicted so it is unclear who-sees-what.** Note that although observations are conducted over time, all temporal data (including time-ordering) is unneeded and unused.

*Example 7.* It is not necessary that the observation support  $\mathcal{O}_\alpha$  contain the observation point associated to  $\alpha \in \mathcal{O}$ . Figure 6 gives an example with feature-based landmarks and observation points which sense via local line-of-sight in a directed cone in the plane. The resulting observation supports still yield a local sensing relation and the various observation and landmark complexes accurately approximate the domain  $\mathcal{D} \subset \mathbb{R}^2$ . One notes that for this class of examples (cones), a higher density of observations (or, equivalently, judicious bearing choices) is required to obtain an accurate approximation of  $\mathcal{D}$ .

*Example 8.* Figure 7 gives an example for which the sensing relation is symmetric: landmarks, endowed with sensing and communication capabilities, observe sufficiently-close neighboring landmarks. In this case,  $\mathcal{O} = \mathcal{L}$ , the sensing relation  $\mathcal{R}$  is symmetric,  $\mathcal{K}_\mathcal{O} = \mathcal{K}_\mathcal{L}$ , and these are homotopic to  $\mathcal{O} = \mathcal{L}$ .

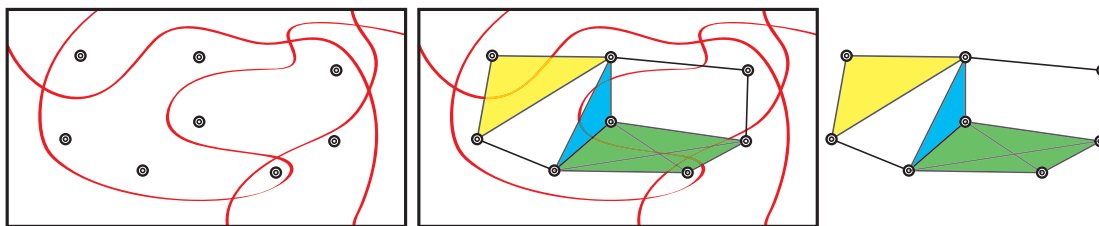


FIGURE 5. Three mobile agents make observations along continuous paths (left); the resulting landmark complex  $\mathcal{K}_L$  (right) and landmark support  $L$  (center) accurately **Rob: here accurately is not really the same as before. In this context we probably need to specify what a hole represents, or?** approximate the region explored by the mobile agents.

It is important to note the differences between this approach and the approach in [12, 13, 31] using Vietoris-Rips complexes of the network. Both methods take as input an undirected graph, connoting communication or visibility. The Vietoris-Rips construction converts this graph into a simplicial complex by means of taking flags or cliques (depending on one's terminology) — the largest simplicial complex with the given graph as 1-skeleton. The present construction is different, in that it uses higher-order intersections to determine simplex membership in  $\mathcal{K}_L$ .

This is a significant modification for two reasons:

- (1) It is impossible to interrogate the topology of the Vietoris-Rips complex by means of Euler characteristic, due to the potential for cross-polytopes and other “fake” generators for homology [12, 13]. The landmark construction, being based on a nerve, avoids this.

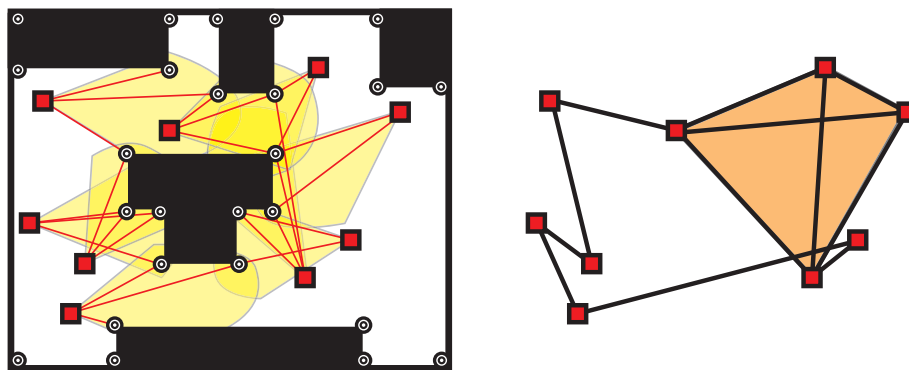


FIGURE 6. A sensing relation based on visibility within a cone is sufficient to yield an accurate approximation of the domain  $\mathcal{D}$ . Note that the observation complex  $\mathcal{K}_O$ , right, has as an abstract complex the homotopy type of a circle, despite the illustrated projection to  $\mathbb{R}^2$ .

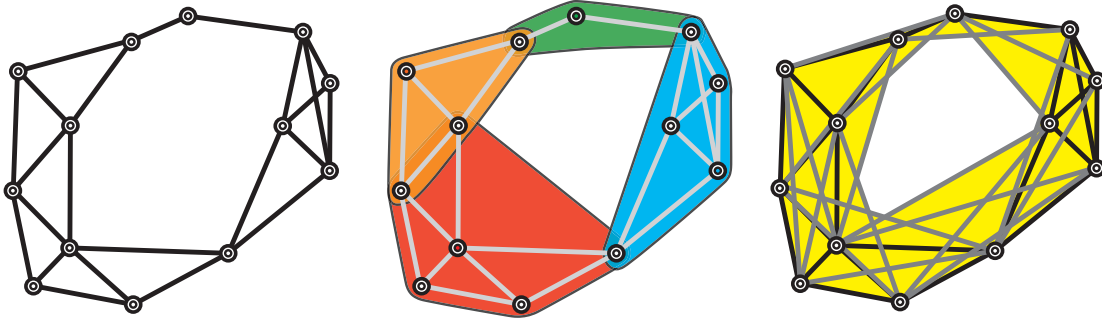


FIGURE 7. A local visibility graph (left) of observer-landmarks (where  $\mathcal{O} = \mathcal{L}$ ) leads to a symmetric visibility relation whose supports (five shown, center) are collectively equivalent to the nerve complex  $\mathcal{K}_{\mathcal{O}} = \mathcal{K}_{\mathcal{L}}$  (right).

- (2) The reason why nerve constructions were not used in [12, 13, 31] stems from the inability to collect sufficient data on depth of coverage, due to the complex nature of overlapping sensor regions.

In the present construction, we assume that the observers have elementary sensing and computation capabilities and can quickly assess and identify landmarks within range. As a result, the present construction, unlike the Vietoris-Rips approach, has no difficulty extending to higher dimensions and requires no complicated “fence” construction [12].

## 7. PERSISTENCE: DISTANCE, NOISE, AND CERTAINTY

The sensing relation has been thus far encoded as binary: yes-or-no detection. Mathematically, this is instantiated by making sensing a relation — a subset  $\mathcal{R}$  of  $\mathcal{O} \times \mathcal{L}$ . We introduce, in the following, a natural but very important enrichment. Instead of modeling sensing as a subset of  $\mathcal{O} \times \mathcal{L}$ , model it as a functional  $\mathcal{R}: \mathcal{O} \times \mathcal{L} \rightarrow \mathbb{R}$ . The binary detection relation has as its image the set  $\{0, 1\} \subset \mathbb{R}$ . More general sensing relations can be integer- or real-valued. Thinking of  $\mathcal{R}$  in this way is akin to controlling the kernel of an integral transform. **Rob: Last sentence is a bit cryptic ... either we say a bit more or remove**

In what follows, we consider the case of slightly richer data in the form of a sensing relation  $\mathcal{R}: \mathcal{O} \times \mathcal{L} \rightarrow \mathbb{R}^+$  that assigns a real non-negative number to each observer-landmark pair. This weight can be used as a proxy for signal strength, distance-to-landmark, or certainty-of-detection. The simple-minded approach to managing such data would be to threshold at a chosen cutoff and construct the complexes of Theorem 4 as desired. However, a more principled approach incorporates recent perspectives from **topological data analysis** [6]. In particular, we propose the use of persistent homology (see §4) as a means of incorporating coarse, noisy distance data into the simplicial constructs of §5.

Specifically, we consider persistent homology and barcodes associated to the following filtered complex. Given  $\mathcal{R}: \mathcal{O} \times \mathcal{L} \rightarrow \mathbb{R}^+$ , choose a finite decreasing sequence in the range  $\{\epsilon_i\}_i \subset \mathbb{R}^+$  as desired. For working with landmark (resp. observation) complexes, consider the filtered simplicial complex  $\emptyset \subset \dots \subset X^i \subset \dots \subset X^j \subset \dots$  defined by constructing the landmark (resp. observation) complex with simplices satisfying  $\mathcal{R} \geq \epsilon_i$  (as opposed to  $\mathcal{R} = 1$  in prior constructs). Because of the decreasing nature of the  $\{\epsilon_i\}$ , the sequence of spaces is connected by inclusions, as per the usual setup for persistent homology.

The following is immediate from the definitions and Theorem 4.

**Corollary 9.** *Under assumptions (A1)-(A5), with a real-valued sensing relation  $\mathcal{R}: \mathcal{O} \times \mathcal{L} \rightarrow \mathbb{R}^+$ , the barcodes associated to the  $\mathbb{R}^+$ -filtered landmark and observation complexes are equal.*

The choice of discretization sequence  $\{\epsilon_i\}$  is arbitrary, so long as the same sequence is used for both landmark and observation complex persistence.<sup>1</sup>

We use signal strength as a persistence parameter, modeling signal strength (arbitrarily) as the reciprocal of distance for purposes of simulation. The benefit of this parameter is that it is often given directly within  $\mathcal{R}$  — the readings come straight from sensors. The examples that follow are from software written to simulate 2-d landmark-based exploration: see §8 for details. Note that in what follows we do not need to consider any known mapping from the persistent parameter to the distance value. This is very desirable as mapping RF-based information to a distance is typically very complex as it strongly depends on the environment, ambient interference, obstacles, etc.

*Example 10.* Figure 8 illustrates 1000 randomly-placed landmarks in the plane with a pair of observers moving along intersecting and self-intersecting paths, sampled evenly for a total of 121 observation points, so that the topology of the observed portion of the plane should have  $H_1$  of rank 2. The sensing relation is  $[0, 1]$ -valued, with value inversely related to distance, as a model of signal strength. The persistent homology of  $\mathcal{K}_0$  filtered by the  $\mathcal{R}$ -weight is computed. Figure 8 shows the lower [left] and upper [middle] thresholds. The resulting barcode for  $H_1$  has two long generators in  $H_1$  and noise at the low end, indicating the presence of two holes in the region explored by the observer. Most interestingly, one of the significant generators [right] is slightly longer than the other [left, middle], and this correlates to the geometry of the holes in the planar regions explored.

*Example 11.* Figure 9 gives an example for which the sensing relation  $\mathcal{R}$  records signal strength, modeled as an inversely proportional to distance-to-landmark. We also added noise to the sensing relation readings — Gaussian and multiplicative with respect to the signal strength (the inverse of distance) at unit mean and 10% standard deviation. The resulting barcode for the first homology group  $H_1$  in Figure 11[right] compares favorably with the ground truth as illustrated, in the sense that the large bars — the large-scale holes — match well.

---

<sup>1</sup>With slightly more sophisticated technology, a continuous parameter may be used without difficulty.

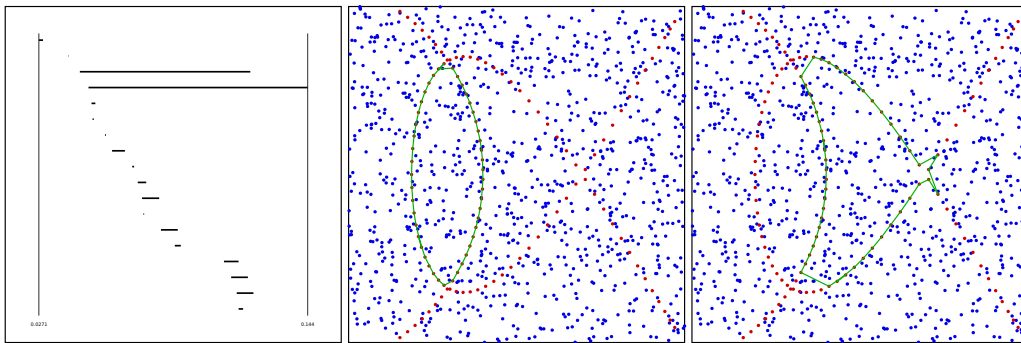


FIGURE 8. Example of signal strength (inversely related to distance) as relation weight. A collection of 1000 landmarks with pair of observers moving along intersecting and self-intersecting paths. The resulting barcode for  $H_1$  [left] has two dominant generators, one [right] longer than the other [left].

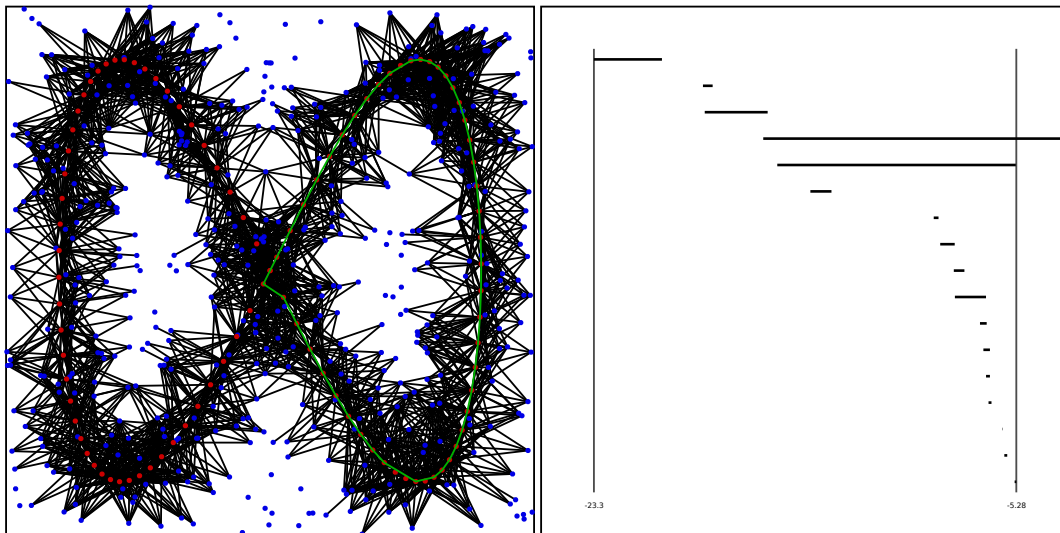


FIGURE 9. Example of signal strength (inversely related to distance) as relation weight, with noise. A collection of landmarks [left] fills a planar domain sampled by observer paths with two holes. The resulting barcode for  $H_1$  [right] has two dominant features.

There is another persistence parameter not seemingly related to distances, but with the ability to capture geometric content. We describe it through an example.

*Example 12.* Figure 11 repeats Example 11 with the same observers, landmarks, and noise. In this case, however, a fixed-distance cutoff is used for a binary  $\mathcal{R}$ , and the (discrete) persistence parameter is chosen to be the *witness weight*. The resulting barcode for the first homology group  $H_1$  in Figure 11[right] compares favorably with that of

Figure 9, in the sense that the large bars — the large-scale holes — match well, whereas the smaller noise-related bars do not correlate.

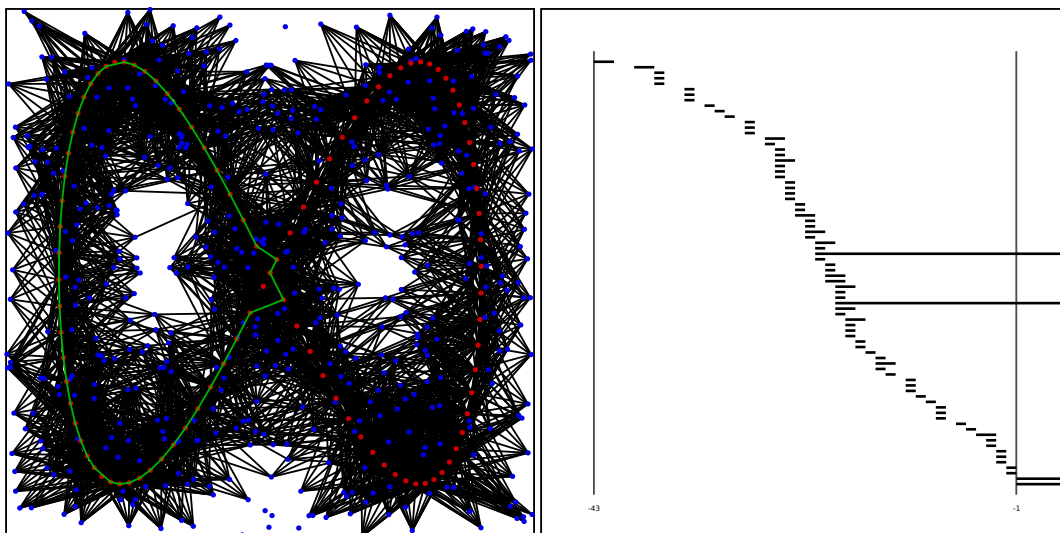


FIGURE 10. A repeat of Figure 9 from Example 11, but using witness weight instead of signal strength as a persistence parameter. Note the preservation of the two dominant features, coupled with the large increase in “topological noise” due to fake generators.

We note in particular that the use of signal strengths, distances, witness weights, or other persistence parameters can provide features that go beyond topological and into geometric descriptors. As an example, the screenshot in Figure ?? shows a setup with two intersecting observer paths, creating a pair of holes in the planar explored domain. One hole is geometrically larger than the other, and this is borne out by comparing the lengths of the associated barcodes. Both bars are long compared to the short noisy features; however, one bar is qualitatively shorter, corresponding to the shorter loop acting a  $H_1$  generator.

Additional examples are given in the following section.

## 8. SIMULATIONS

Our algorithms for constructing a chain complex from the sensing relation  $\mathcal{R}$  are straightforward. In all our simulations, we are working with landmarks and observations in a subset of the Euclidean plane, and, as such, are content to use the homology groups  $H_0$  and  $H_1$  to detect, respectively, connectivity and holes-in-the-plane: these completely characterize the topology (homotopy type) of the observed subspace. Given  $\mathcal{R}$ , we employ a sweeping algorithm to construct the simplicial structure of the complexes  $\mathcal{K}_0$  or  $\mathcal{K}_{\mathcal{L}}$  (usually the former, as being smaller). The computational complexity of building

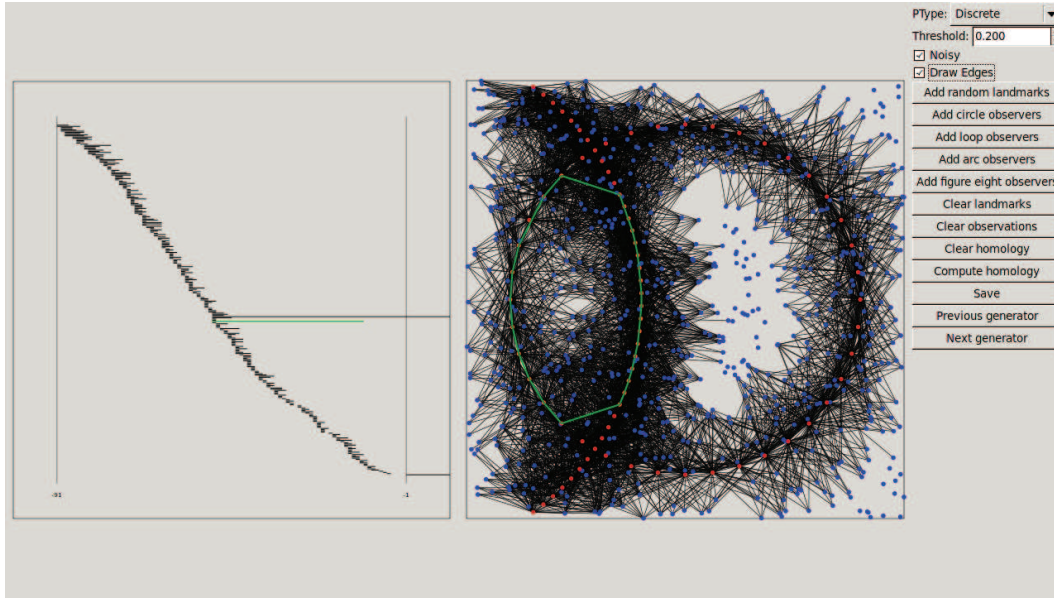


FIGURE 11. Screenshot of software for computing the homology of  $\mathcal{K}_0$ .

the chain complex for  $\mathcal{K}_0$  or  $\mathcal{K}_L$  is certainly combinatorial in general (classical curse-of-dimensionality). However, to compute  $H_1$  requires only the construction up to and including cells of dimension 2. The construction of the 2-skeleton from a dense  $n$ -by- $k$  relation  $\mathcal{R}$  is of time complexity  $O(nk^3)$ . Sparsity of  $\mathcal{R}$  impacts the  $k$  factor (and thus has a dramatic impact).

The program that produced these examples was written in C++, and uses GTK+ for its graphical output. Its primary purpose is to compute the persistent homology in grading 1 of the observation complex  $\mathcal{K}_0$  associated to a configuration of landmarks and observations. It computes not only the persistent homology but also explicit and efficient generators thereof, and incorporates a GUI for inputting observations, specifying the sensing relation, and adding noise.

In order to compute 1-dimensional persistent homology, it is sufficient to construct the 2-skeleton of the observation complex (the subcomplex consisting of 0-, 1-, and 2-dimensional simplices only). Thus, for each landmark  $i \in \mathcal{L}$ , we first find the set  $\mathcal{R}^i = \{\alpha \in \mathcal{O} : (\alpha, i) \in \mathcal{R}\}$ . In several of the examples shown below,  $(\alpha, i) \in \mathcal{R}$  if and only if the distance between the associated observation point and landmark point is within some fixed threshold. We then iterate over all subsets of  $\mathcal{R}^i$  of cardinality 1, 2, or 3, and add these to the observation complex as vertices, edges, or 2-simplices, respectively. As we do this, we keep a running count of the number of times a given simplex has been added (for witness weight persistence) or a running minimum of the distances at which a given simplex is 'connected up' by a given landmark (for signal-strength persistence). Once we have built the observation complex and associated a persistence parameter to each simplex, we compute the persistent homology using

the algorithm of Zomorodian-Carlsson [35], with minor modifications to adapt to the encoding of the simplicial complexes in  $\mathcal{R}$ .

*Example 13.* Figure 12 illustrates 1000 randomly-placed landmarks in the plane with 40 observation points arranged around a circle, so that the topology of the observed portion of the plane should have  $H_1$  of rank 1. The sensing relation is  $\{0, 1\}$ -valued based on a fixed distance. The persistent homology of  $\mathcal{K}_O$  filtered by the witness-weight is computed. Figure 12 shows the lower [top] and upper [bottom] thresholds, with observations [left] and simplicial constructions [right]. The resulting barcode for  $H_1$  has one long generator and noise at the low end, indicating the presence of a single hole in the region explored by the observer.

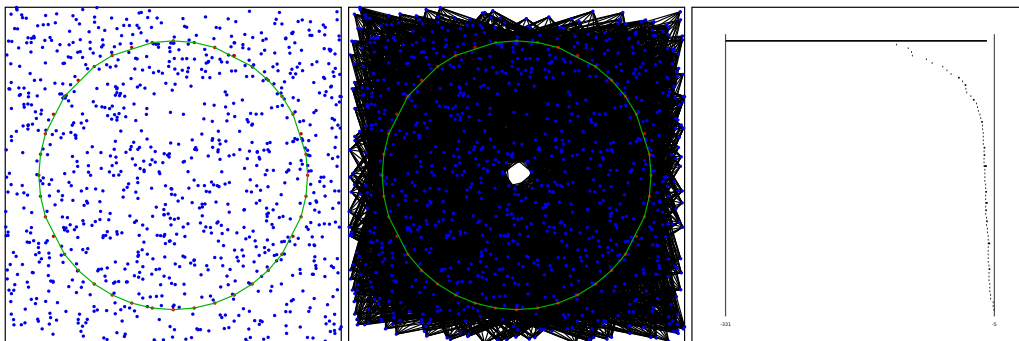


FIGURE 12. Example of fixed-distance sensing, filtered by witness-weight. A collection of 1000 landmarks with a single observer moving in a circular path generates a filtered observation complex on 40 observation points. The resulting barcode for  $H_1$  has one dominant feature.

## 9. SNEAKING AND MISIDENTIFIED LANDMARKS

The settings considered thus far involve static landmarks and observations. It would seem that interrogating domain topology/geometry from a collection of observations of non-localized moving landmarks with no time registration or model of movement is impossible, as independent observations of landmark configurations cannot be correlated. However, some progress can be made in the context of partial landmark mobility. This setting — which we will refer to as **landmark sneak** — envisions an ensemble of landmarks  $\mathcal{L}$  whose positions  $|\mathcal{L}|$  in  $\mathcal{D}$  are by-and-large fixed, but with a reasonably small subset of  $\mathcal{L}$  *sneaking* about. The observers cannot distinguish between the fixed and sneaking landmarks. The problem of how to construct a topologically-accurate model of  $\mathcal{D}$  or the observer motion paths from the sensory observations  $\mathcal{R}$  is nontrivial, as the following example shows.

*Example 14.* Figure 13 gives an example with a single observer moving along a circular path in  $\mathcal{D} = \mathbb{R}^2$  and taking periodic observations, sensing landmarks within a fixed distance. The various landmark and observation complexes correctly reconstruct the



topology of the annular portion of  $\mathcal{D}$  sensed by the observer. However, a single sneaking landmark is enough to modify the topology of the landmark and observation complexes to a nearly arbitrary degree. The observer, upon seeing the sneaking landmark again, believes itself to have revisited a neighborhood of the observer's path. This observation has the effect of gluing together metrically-far regions of  $\mathcal{D}$  in the simplicial approximation.

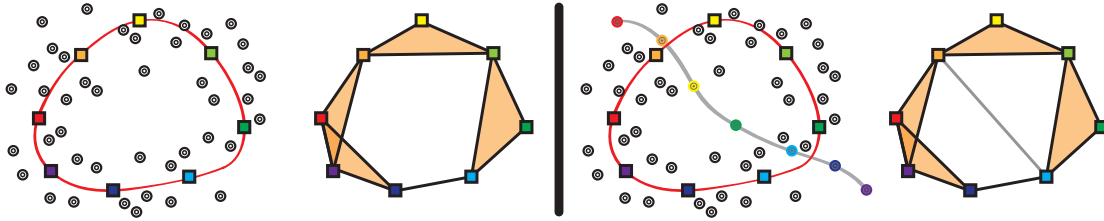


FIGURE 13. A single observer travels using a sensing relation based on distance. With fixed landmarks [left], the complex  $\mathcal{K}_0$  correctly reconstructs the annular path. A single sneaking landmark [right] is enough to trick  $\mathcal{K}_0$  into thinking that geometrically far observation points are close, thus ruining the topology approximation.

In the context of multiple observers moving along paths in  $\mathcal{D}$ , sneaking landmarks can trick the observation complex into believing that the observers have crossed paths in  $\mathcal{D}$  when in fact they have not. Note that the addition of a sneaking landmark impacts the topology of the observation/landmark complexes in one direction — it adds simplices, but cannot subtract. Our proposed strategy for correcting the topology consists of eliminating the spurious simplices added by sneaking.

Weights can be used to filter out spurious simplices caused by sneaking landmarks as follows. If we assume that (1) sneaking landmarks form only a small fraction of the total landmark population, or (2) sneaking landmarks do not move collectively in groups, then the weight of any spurious simplex will be small.

*Example 15.* Figure 14 gives an example for which the sensing relation is determined by distance to a mobile observer traveling along a circular path in  $\mathbb{R}^2$ . The construction of  $\mathcal{K}_0$  is illustrated with edge thickness corresponding to weight  $w$ . In this example, the grey 2-simplex in Figure 14[right] arises because two sneaking landmarks travel in tandem and appear together to an observer at two different times and places. However, the weight of this 2-simplex (and two of its supporting edges) is 1, far less than the weights of the other edges used to generate the topology of the observer's domain of exploration.

*Example 16.* Figure 15[left] illustrates a simulation with 500 randomly-placed landmarks for which the sensing relation is binary and determined by a fixed distance-to-landmark. Two mobile observers travel along intersecting and self-intersecting paths,

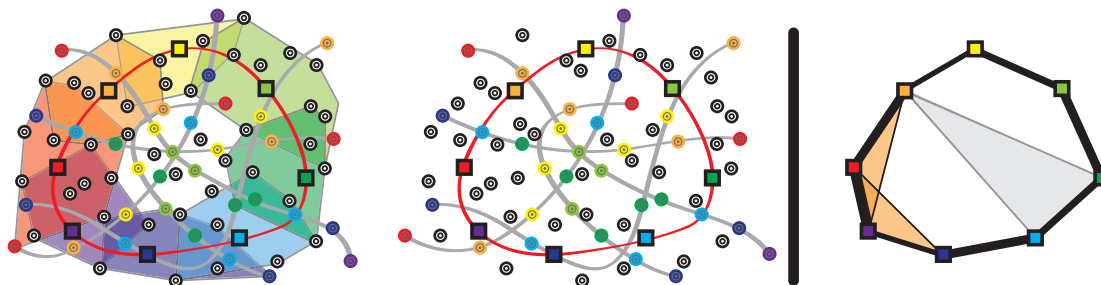


FIGURE 14. An observer moves in time along a circular path [left], registering landmarks by distance. A large number of sneaking landmarks try to confuse the observer [middle] and indeed lead to one spurious 2-simplex in  $\mathcal{K}_0$  [right]. By thresholding according to weight, the undesired 2-simplex is removed, leaving an accurate approximation to the path of the observer.

and are sampled evenly with 121 observation points. There is one “sneaking” landmark that moves along a circular path, oriented oppositely to the incident mobile observer. Without the use of witness weight to filter the complex, there exists a generator [top, left] for  $H_1(\mathcal{K}_0)$  that corresponds to a “false” hole caused by seeing the sneaking landmark twice and believing to be in the same location at each time. Using witness weight as a persistence parameter reveals the existence of two long barcodes in  $H_1$  [lower left]. The spurious generator for  $H_1$  caused by low-witness weight, illustrated in Figure 15 [right] is short in the barcode representation, coming into view only at witness weight equal to 1.

The problem of misidentified stationary landmarks is equivalent and of more direct relevance to mapping. In the analogy of the wandering traveler used in the introduction to this paper, certain landmarks on city streets can be ambiguous, due to misidentification (“*I went left at the wrong pub*”) or ubiquity (“*I saw this brand of coffee shop before, but was I at this one then?*”). Filtering by witness weight is again a simple means of removing some of the ambiguity. The risk, of course, is that filtering out low-witness-weight simplices may also remove genuine simplices with low weight resulting from an undersampling of the domain in terms of landmark density.

## 10. CONCLUSIONS

This work suggests a number of ways to create topologically faithful maps of an environment based on a collection of observations of identifiable landmarks, with or without coarse range data. The principal technical results concern various dualities and equivalences between observation/landmark complexes/supports; such permit the free exchange of one simplicial system for another, where appropriate for reasons of parsimonious representation or geometric motivation. In many applications, however, the observation complex (using observation points as vertices) is most natural and the

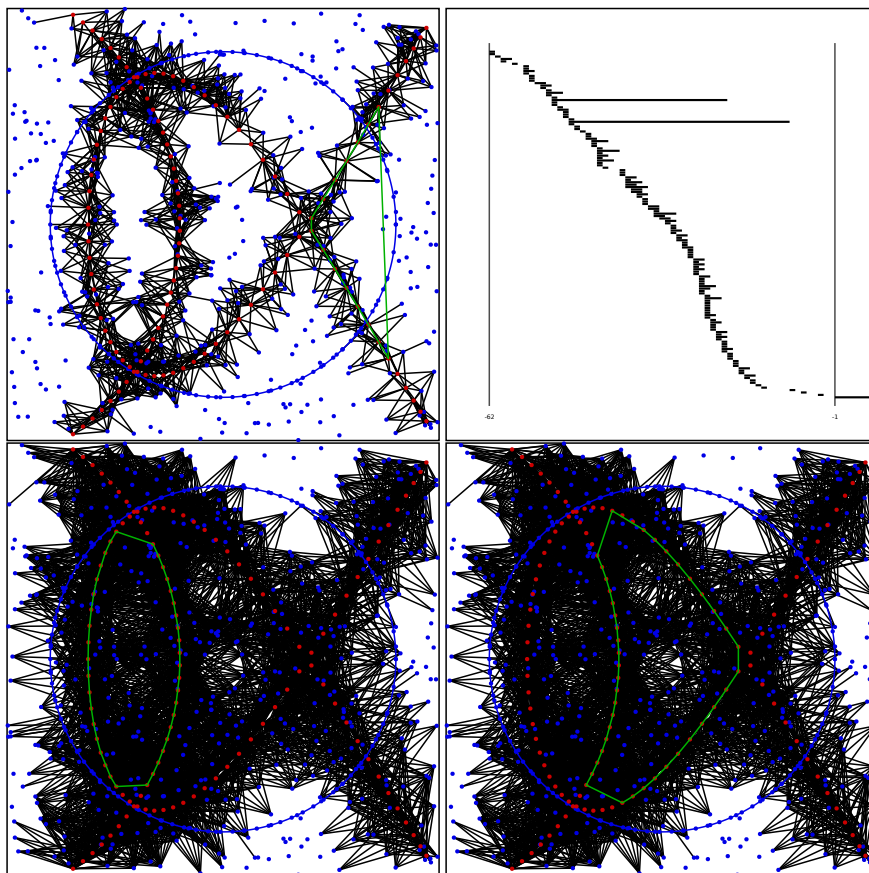


FIGURE 15. A collection of 500 landmarks with pair of observers moving along intersecting and self-intersecting paths. There is a ‘fake’ generator for  $H_1(\mathcal{K}_0)$  [upper left], but performing a persistence computation on witness weight reveals a barcode for  $H_1$  [top, right] with two significant bars, not three. The two significant generators of  $H_1$  [lower] identify the observed portion of the plane.

one to be constructed. This paper demonstrates the utility of using homology (for binary sensing relations) and persistent homology (for real-valued or intensity sensing relations) for estimating the topology of the domain sampled by the observation points.

In the context of the envisaged applications — in which several vehicles move independently through an unknown domain without GPS, odometry, or other metric-based sensing — the techniques of this paper can be used to reconstruct the regions explored, even in the context of misidentified landmarks, mobile landmarks, or vehicles that cross paths in space at different times.

## REFERENCES

- [1] P. Alexandrov, "Simpliziale Approximationen in der Allgemeinen Topologie," *Math. Ann.* 96, 489–510, 1927.
- [2] R. Atkin, "An Algebra for Patterns on a Complex, I," *Int. J. Man-Machine Studies* 6, 1974, 285–307.
- [3] R. Atkin, "An Algebra for Patterns on a Complex, II," *Int. J. Man-Machine Studies* 8, 1976, 483–448.
- [4] A. Björner, "Topological Methods," in *Handbook of Combinatorics*, Vol. 2, Ch. 34, 1995.
- [5] M. Bridson and A. Haefliger, *Metric Spaces of Nonpositive Curvature*, Springer-Verlag, 1999.
- [6] G. Carlsson, "Topology and Data" , *Bull. Amer. Math. Soc.*, 46:2, 2009, 255–308.
- [7] E. Čech, "Théorie générale de l'homologie dans un espace quelconque," *Fund. Math.* 19, 149–183, 1932.
- [8] P. Cheeseman and P. Smith, "On the representation and estimation of spatial uncertainty." *International Journal of Robotics* 5, 56–68, 1986.
- [9] H. Choset and K. Nagatani, "Topological simultaneous localization and mapping (SLAM): Toward exact localization without explicit localization," *IEEE Trans. Robot. Autom.*, 17(2), 125–137, 2001.
- [10] C. Curto and V. Itskov, "Cell groups reveal structure of stimulus space," *PLoS Computational Biology* 4(10), 2008. e1000205. doi:10.1371/journal.pcbi.1000205
- [11] V. de Silva and G. Carlsson. "Topological estimation using witness complexes," in *SPBG04 Symposium on Point-Based Graphics*, 2004, 157-166.
- [12] V. de Silva and R. Ghrist, "Coordinate-free coverage in sensor networks with controlled boundaries via homology," *Intl. J. Robotics Research*, 25:12, 2006, 1205–1222.
- [13] V. de Silva and R. Ghrist, "Coverage in sensor networks via persistent homology," *Alg. & Geom. Top.*, 7, 2007, 339–358.
- [14] C. Dowker, "Homology groups of relations," *Ann. Math.* 56:1, 84–95, 1952.
- [15] H. Durrant-Whyte and T. Bailey, "Simultaneous localization and mapping: part I," *IEEE Robotics & Automation Magazine*, 13:2, 99–110, 2006.
- [16] H. Edelsbrunner and J. Harer, *Computational Topology: an Introduction*, AMS, 2010.
- [17] N. Fairfield, G. Kantor, and D. Wettergreen, "Real-Time SLAM with Octree Evidence Grids for Exploration in Underwater Tunnels." *J. Field Robotics*, 24: 3–21, doi: 10.1002/rob.20165, 2007.
- [18] R. Ghrist, "Barcodes: The persistent topology of data," *Bull. Amer. Math. Soc.*, 45:1, 2008, 61–75.
- [19] R. Ghrist, H. Owen, and M. Robinson, "DTIME: Discrete topological imaging for multipath environments," Penn ESE Technical Report, 8-1-2010.
- [20] A. Hatcher, *Algebraic Topology*, Cambridge University Press, 2002.
- [21] D. Haussler and E. Welzl, "Epsilon-nets and simplex range queries." In *Proc. 2<sup>nd</sup> Ann. Symp. Comp. Geom. (SCG '86)*. ACM, New York, NY, USA, 61-71, 1986.
- [22] D. Huber and N. Vandapel, "Automatic Three-dimensional Underground Mine Mapping," *Intl. J. of Robotics Research*, 25(1), 7–17, 2006.
- [23] J. Leonard and H. Durrant-Whyte, "Mobile robot localization by tracking geometric beacons." *IEEE Transactions on Robotics and Automation* 7(3):376–382, 1991.
- [24] J. Leray, "Sur la forme des espaces topologiques et sure les points fixes des représentations," *J. Math. Pures Appl.*, 24, 95–167, 1945.
- [25] E. Lobaton, R. Vasudevan, R. Bajcsy and S. Sastry, "A distributed topological camera network representation for tracking applications," *IEEE Trans. Image Proc.* 19(10), 2516–2529, 2010.
- [26] M. Montemerlo and S. Thrun, *FastSLAM: A Scalable Method for the Simultaneous Localization and Mapping Problem in Robotics*, Springer-Verlag, Berlin Heidelberg, 2007.
- [27] J. Munkres, *Elements of Algebraic Topology*, Westview Press, 1984.
- [28] P. Niyogi, S. Smale, and S. Weinberger, "Finding the homology of submanifolds with high confidence from random samples." *Discrete Comput. Geom.* 39, 1, 2008, 419-441.
- [29] V. Robins, "Computational Topology for Point Data: Betti Numbers of  $\alpha$ -Shapes," in *Morphology of Condensed Matter, Lecture Notes in Physics*, Volume 600, 2002, 261-274.
- [30] S. Shen, N. Michael, and V. Kumar, "Autonomous indoor 3-D exploration with a micro-aerial vehicle." In *Proc. of the IEEE Intl. Conf. on Robot. and Autom.*, 2012.

- [31] A. Tahbaz Salehi and A. Jadbabaie. Distributed coverage verification in sensor networks without location information. *IEEE Transactions on Automatic Control*, 55(8), August 2010.
- [32] T. Tao, S. Tully, G. Kantor, H. Choset, "Incremental construction of the saturated- GVG for multi-hypothesis topological SLAM." In *Proc. ICRA 2011*, 3072–3077, 2011.
- [33] A. Tapus and R. Siegwart, "Topological SLAM using Fingerprints of Places", In P. Bessière, R. Siegwart and C. Laugier, eds., *Probabilistic Reasoning and Decision Making in Sensory-Motor Systems*, Vol. 46, Springer-Verlag, 99–12 , 2008.
- [34] S. Thrun, *Probabilistic Robotics*, MIT Press, 2009.
- [35] A. Zomorodian and G. Carlsson , "Computing persistent homology," *Disc. Comput. Geom.* 33:2, 2005, 247–274.

DEPARTMENTS OF MATHEMATICS AND ELECTRICAL/SYSTEMS ENGINEERING, UNIVERSITY OF PENNSYLVANIA, PHILADELPHIA PA, USA

*E-mail address:* ghrist@math.upenn.edu

DEPARTMENT OF MATHEMATICS, UNIVERSITY OF PENNSYLVANIA, PHILADELPHIA PA, USA

*E-mail address:* dlipsky@math.upenn.edu

UNITED TECHNOLOGIES RESEARCH CENTER, EAST HARTFORD, CT, 06108

UNITED TECHNOLOGIES RESEARCH CENTER, EAST HARTFORD, CT, 06108